The Effect of Oceanic Isoprene Emissions on Secondary Organic Aerosol Formation in the Coastal United States

Brett Gantt, Nicholas Meskhidze*, Yang Zhang, and Jun Xu
Department of Marine, Earth, and Atmospheric Sciences
North Carolina State University, Raleigh, NC

1. INTRODUCTION

Isoprene (C_5H_8) is the most ubiquitous biogenic volatile organic carbon (BVOC) with annual global emissions estimated of 500 to 750 Tg of carbon (Guenther et al., 2006). Emission inventories for terrestrial sources of isoprene have been created using parameters such as tree species, leaf area index, and change of incoming radiation. In addition to terrestrial sources, isoprene emissions have also been measured over the productive areas of the world's oceans, particularly in the vicinity of large phytoplankton blooms. Laboratory measurements for the isoprene production from five different species of plankton show that for a given environmental condition, diatoms have the highest emission rates followed by dinoflagellates, cyanobacteria, and coccolithophores (Shaw et al., 2003). Annual global oceanic isoprene emissions are estimated to be between 0.12 and 2.7 Tg of carbon when using the bottom up inventories (Palmer and Shaw, 2005; Matsunaga et al., 2002) and ~2 Tg of carbon when using the top down modeling (Arnold et al., 2008).

In the troposphere, isoprene reacts with hydroxyl radicals (OH), ozone (O_3), and nitrate radicals (NO_3). Owing to its high concentration and reactivity with OH radicals, isoprene plays an important role in the photochemistry occurring within the atmospheric boundary layer. The photooxidation of isoprene can also lead to the formation of low volatility species that condense to form secondary organic aerosols, SOA (Claeys et al., 2004; Edney et al., 2005). The SOA yields (defined as the ratio of the mass of SOA formed to the mass of isoprene reacted) under nitrogen oxide (NO_x)-free conditions have been observed to be as high as 3% (Kroll et al., 2006). Additional laboratory chamber studies suggest SOA yields from 0.2% to 24% (Edney et al., 2005; Ng et al., 2008), while the aqueous phase chemical processes may lead to an SOA yield between 0.4% to 42% (Ervens et al., 2008).

Despite the relatively small contribution of estimated marine isoprene emissions to the global scale isoprene flux, the contributions of marine sources to the regional isoprene budget and SOA burden are poorly defined. In this study, we examine marine isoprene emissions and the subsequent contributions to the SOA mass concentrations at the coastal regions of the United States. Coastal and coastally influenced waters make up only 10% of the ocean surface area; however, due to their high productivity these waters are likely to make up the major fraction of the global marine trace gas flux (Butler et al., 2007).

2: METHOD

To determine the influence of marine isoprene emissions on SOA formation, we have conducted the Community Multi-scale Air Quality (CMAQ) model simulation using a 36 x 36 km^2 spatial resolution in a domain encompassing the continental US and parts of southern Canada and northern Mexico. The meteorology is generated using Pennsylvania State University/National Center for Atmospheric Research Mesoscale Modeling System Generation 5 (MM5) Version 3.6.1 using four-dimensional data assimilation. The simulations start on July 1st, 2001 using the output from the one year CMAQ run of Zhang et al., (2007) and the boundary conditions are set from GEOS-Chem every 3 hours (Park et al., 2004). Primary emissions of anthropogenic gaseous and aerosol species and terrestrial isoprene emissions are based on the 2001 National Emissions Inventory (NEI) from the U.S. Environmental Protection Agency (US EPA) for anthropogenic emissions and the U.S. EPA's Biogenic Emissions Inventory System (BEIS) version 3.12 for biogenic emissions. SOA formation from isoprene is modeled in CMAQ using the isoprene addition to the Carbon-Bond

---

*Corresponding Author: Nicholas Meskhidze, Department of Marine, Earth, and Atmospheric Sciences, NCSU, 2800 Faucette Dr., Raleigh, NC 27695; e-mail: nicholas_meskhidze@ncsu.edu

Mechanism version IV (CBM-IV) described in Zhang et al. (2007).

Modeling of isoprene emissions requires knowledge of the emission rates for a given amount of chlorophyll *a,* [Chl *a*] and light intensity. Laboratory measurements of isoprene concentrations for different species of phytoplankton were conducted using headspace gas chromatography. To assess the effect of changing incoming solar radiation for isoprene production, the plankton was exposed to various levels of light intensity. The ambient conditions were simulated using light intensities ranging from 0 to 1500 μE/m^{2}s (~0 to 1000 W/m^2), characteristic to summertime conditions at the North American coast. Our measurements show that production rates typically increase under increasing light intensity. As a result, isoprene production rates used in this study are significantly higher compared to previous studies using a lower maximum light intensity of 200 μE/m^{2}s (~133W/m^2). Isoprene production is estimated using a positive linear relationship with the incoming light:

$$P = 0.002I - 0.3 \qquad (1)$$

where P is the production in μmoles isoprene produced (g chlorophyll *a*)$^{-1}$ hr^{-1} and I is the incident solar radiation in W/m^2. Both the slope and intercept for this equation are derived from measurements of the diatom *Thalassiosira weissflogii* which is used to represent phytoplankton speciation for the coastal US. To calculate total isoprene emission rates from a given model grid cell, we multiply P values (derived per unit mass of [Chl *a*]) by remotely sensed [Chl *a*]. Surface [Chl *a*] was derived from the Sea-viewing Wide Field-of-view Sensor (SeaWiFS) satellite since it has been shown to have an accurate retrieval of in situ chlorophyll concentrations in coastal sites (Blondeau-Patissier et al., 2004). The level 3, monthly-averaged surface [Chl *a*] data for July 2001 (originally in ~9 x 9 km^2 spatial resolution) were regridded to a 36 x 36 km^2 and geographically projected into the Lambert Conformal Conic coordinates. Figure 1 shows the [Chl *a*] within the coastal areas of the continental U.S.

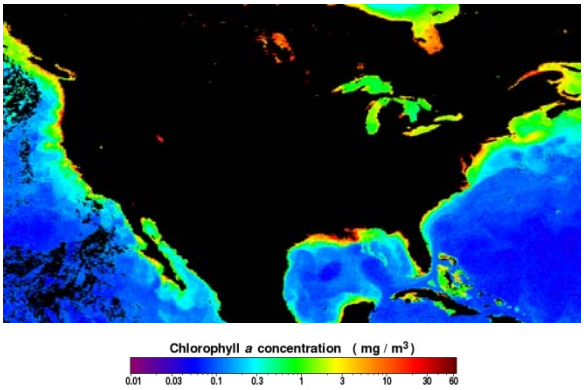

Figure 1. Spatial distribution of the monthly SeaWiFS-derived [Chl *a*] during July 2001 for the continental U.S. coastal waters. The warmer colors showing the highest concentrations located in near-coastal waters and inland lakes.

The amount of solar radiation received by phytoplankton at different depths of the water column is calculated using surface incoming solar radiation (from CMAQ) and the light attenuation is estimated using Beer-Lambert's Law: $T = e^{-k\,d}$. Here T is transmittance fraction, k is the diffuse attenuation coefficient, and d is the actual depth of the water. The level 3, monthly-averaged values of k (at 490 nm wavelength) for July 2001 were downloaded from SeaWiFS and regridded in a way similar to [Chl *a*]. To account for the effect of decreasing light intensity on isoprene production rates, every horizontal grid of the ocean surface was divided into 14 exponentially increasing vertical sub-layers. The maximum depth of the layer was determined by the point at which the transmittance fraction equals to 0.1 (i.e., point where 90% of absorption is reached). The isoprene production for each vertical sub-layer of the model horizontal domain is inferred using Eq. 1 with the available light intensity (I) calculated at the midpoint of each sub-layer.

The total column isoprene production is found by taking the sum of all 14 vertical sub-layers. Since isoprene is highly insoluble in water and the air-sea exchange is the primary pathway for isoprene loss within the water column (Palmer and Shaw, 2005), it is assumed that all ocean-produced isoprene is directly vented into the atmosphere.

Three separate monthly (for July 2001) simulations are carried out using different isoprene emission schemes: 1) terrestrial emissions only, 2) terrestrial and marine emissions, and 3) terrestrial and marine emissions, with marine emissions increased

five-fold over the calculated values. This later simulation with elevated emissions is designed to test the sensitivity of isoprene and SOA mass concentrations from marine isoprene emissions due to daily and seasonal variations in [Chl *a*].

3. RESULTS

In order to estimate the maximum impact of marine isoprene emissions on isoprene and SOA mass concentrations, three regions near productive oceans were selected for temporal analyses. The spatial extent of the selected regions is shown in Figure 2.

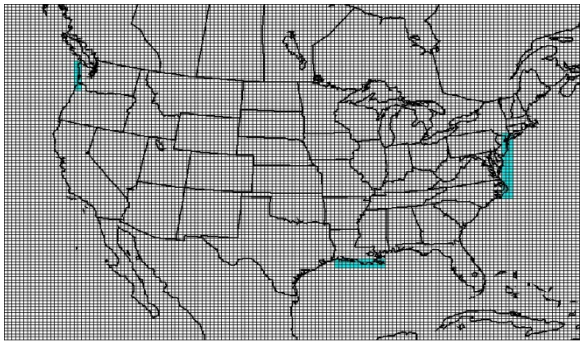

Figure 2. CMAQ model domain and the smaller regions (highlighted in blue) selected for the analyses due to their proximity to productive oceans. These areas are defined from left to right as 1) Washington coast, 2) Louisiana coast, and 3) Mid-Atlantic coast.

The 8-day period from July 19th to July 26th shown on Figure 3 was arbitrarily selected to demonstrate the diurnal variations in marine emissions of isoprene. The light sensitivity of isoprene production results in an emission pattern that follows the pattern of solar radiation. Inspection of Figure 3 shows that for each region, marine isoprene emissions begin at approximately 9 am local time, reach a maximum at 2 pm, and diminish around 8 pm. This pattern of marine isoprene emissions is consistent with one shown by Sinha et al. (2007). Emission rates were the highest near the Louisiana coast, with average values up to 0.06 mole/s per grid cell. Both the mid-Atlantic and Washington coasts had maximum daily-average emissions of 0.03 moles/s per grid cell. These rates are somewhat higher, but consistent with phytoplankton produced isoprene (hereinafter referred as marine-source isoprene) emission rates in the mesocosms off the coast of Norway (Sinha et al., 2007) When extrapolated to the 36 x 36km^2 CMAQ grid cell, marine-source isoprene emission rates at the Norwegian coast were ~ 0.02 moles/s. Figure 4 shows the spatial distribution of simulated monthly averaged midday marine isoprene emissions, with the highest rates located in the Gulf of Mexico, characterized by high [Chl *a*] and solar radiation.

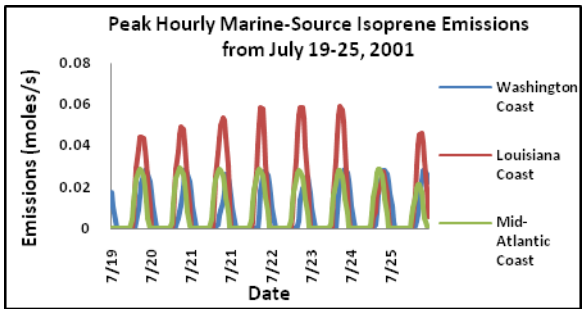

Figure 3. Peak hourly marine isoprene emissions from the three selected regions.

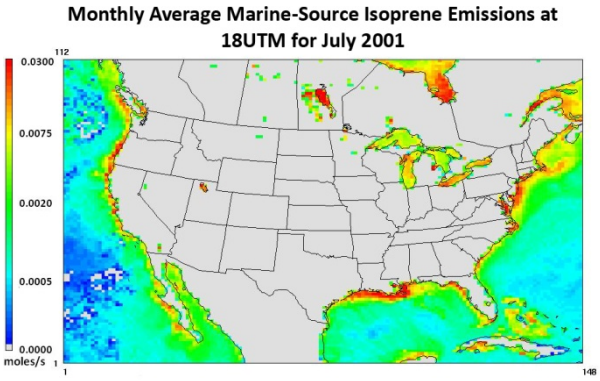

Figure 4. Monthly averaged marine isoprene emissions for 18 UTM during July 2001.

Contribution of marine-source emissions to boundary layer isoprene concentrations and SOA formation were determined by taking the differences in the outputs between the simulation with marine isoprene sources and the simulation with only terrestrial sources of isoprene. Isoprene concentrations in the lowest CMAQ layer (surface to 35 meters) closely follow the diurnal cycle of isoprene emissions with the peak values in the early afternoon and the minimum values in the early morning. Figure 5 shows peak daily concentrations of 25 parts per trillion (ppt) for the Washington coast, 20 ppt for the Louisiana coast, and 12 ppt for the Mid-Atlantic coast.

Isoprene concentrations vary widely from day to day in each of the three regions with afternoon concentrations changing by about a factor of 3. The highest concentrations occur along the Washington coast because of the longer fetch over high [Chl *a*] waters. These

peak values are lower than recently observed isoprene concentrations in marine air at stations on the coasts of Greece, Norway, and Ireland, where concentrations as high as 60, 180, and 68 ppt were measured (Liakakou et al., 2007; Sinha et al., 2007; Greenberg et al., 2005). The reasons for the discrepancy between our model-simulated and observed concentrations could be the influence of terrestrial isoprene sources at measurement sites and/or the difficulties associated with the comparison of the model grid area-averaged values with in-situ point measurements.

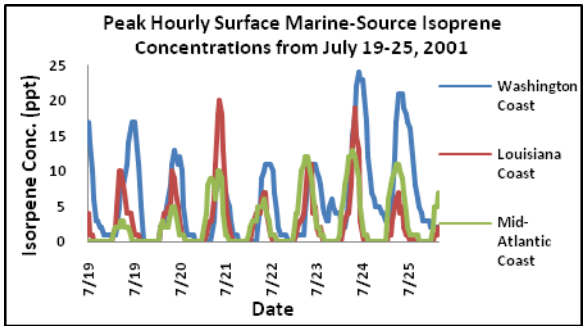

Figure 5. Peak hourly marine-source isoprene concentrations within selected regions.

Figure 6 shows that the maximum marine-source isoprene contribution to SOA mass concentration is approximately 7 ng/m^3 along the Washington coast, 4 ng/m^3 along the Mid-Atlantic coast, and 1 ng/m^3 on the Louisiana coast. One possible reason for the relatively low SOA mass concentrations near the Louisiana coast is the higher ambient temperatures that may lead to different partitioning of the isoprene oxidation products (Pankow, 1994). Due to background biogenic SOA mass concentrations often higher than 10 µg/m^3 in some inland locations, the contribution of marine-source isoprene to SOA mass concentration is non-trivial only in coastal areas.

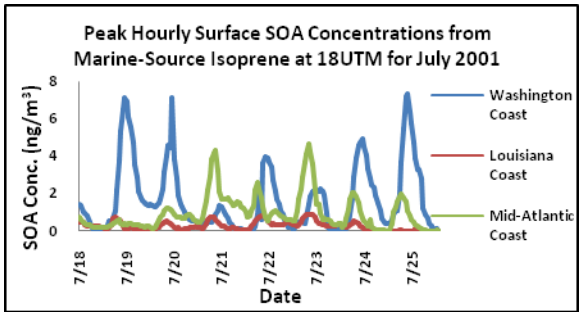

Figure 6. Peak hourly marine-source isoprene-derived SOA mass concentrations within selected regions.

To account for the inter-annual variability of [Chl *a*] and the uncertainties in phytoplankton isoprene production, we ran a third simulation with marine-source isoprene emissions increased by a factor of 5. Figure 7 shows the midday spatial distribution of changes in SOA mass concentration due to amplified marine-source isoprene emissions. All coastal locations have small increases in SOA mass concentration as a result of marine isoprene emissions, with the largest inland changes occurring in the near the coast of the Pacific Northwest.

In the Pacific Northwest and California, marine-source isoprene emissions can result in a slight increase in the SOA mass concentrations hundreds of miles from the coast. Inland areas near the Great Lakes region also experience slight increases in SOA mass concentrations due to the nearby emission source. Besides these isolated areas, very few inland areas in the Continental U.S. experience any considerable change in SOA mass concentration due to marine-source isoprene.

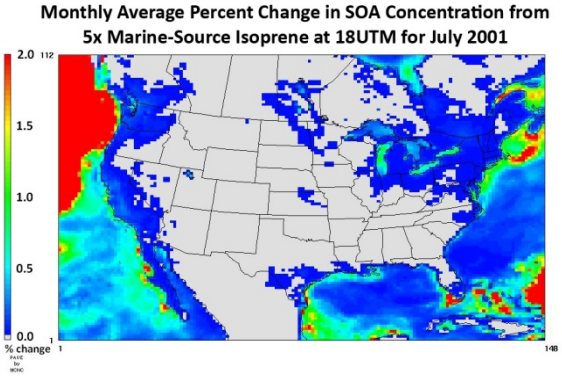

Figure 7. Monthly-average contribution of marine-source isoprene to SOA mass concentrations for July 2001 at 18 UTM. Locations in red have changes 2% or greater, with some areas in the remote ocean having greater than a 100% increase.

In addition to its ability to oxidize into SOA precursors, isoprene can also enhance ozone (O_3) production through the formation of formaldehyde (HCHO). Figure 8 shows the midday spatial distribution of changes in O_3 concentrations due to amplified marine-source isoprene emissions. This figure shows that the increases in O_3 concentrations are greatest over the mid-Atlantic and New England states. The distribution of changes in O_3 concentrations is different than that of SOA because NO_x concentrations play a major role in O_3 formation

while not affecting SOA formation in CMAQ. Overall, the percent increases in O_3 concentration are very small; the majority of coastal areas are experiencing less than a 0.1 % increase in O_3 concentrations as a result of marine-source isoprene emissions.

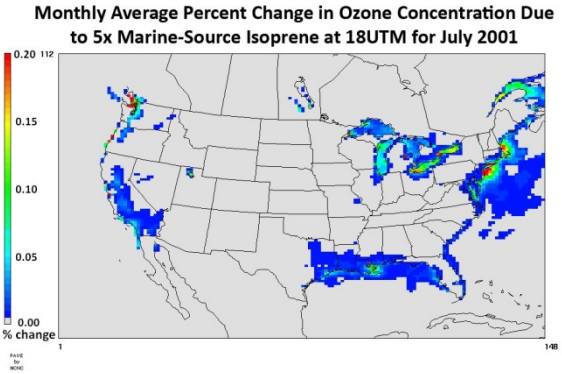

Figure 8. Monthly-average contribution of marine-source isoprene-derived O_3 concentrations for July 2001 at 18 UTM.

4. CONCLUSION

This study simulates diurnal variations of marine-source isoprene emissions and its effects on concentrations of isoprene, SOA, and O_3. Here, for the first time, using new laboratory measurements of isoprene production by phytoplankton under a range of light conditions, we simulate concentrations of marine-source isoprene and SOA comparable to observations. However, the simulated changes in total SOA and O_3 concentrations due to marine-source isoprene were small. Despite this fact, the importance of marine-source isoprene for coastal SOA and O_3 formation cannot be discarded due to smoothing of highly localized coastal emissions over the 36 x 36 km^2 grid and large uncertainties in the dry and aqueous isoprene-SOA yields.

To model marine-source isoprene emissions more accurately, better understanding of the mechanism responsible for phytoplankton emitted isoprene is needed. Also future modeling studies should be done at lower spatial grid resolution to capture localized high emissions. Estuaries, for example, are very productive water bodies with a spatial extent far less than the 36 x 36 km^2 CMAQ grid employed in this study. These high isoprene-emitting areas would have better emission estimates with estuary-level [Chl *a*] data and higher spatial resolution from CMAQ.

ACKNOWLEDGEMENTS

This research was supported by the Office of Science (BER), U.S. Department of Energy, Grant No. DE-FG02-08ER64508. The baseline CMAQ simulation without marine isoprene emissions was conducted with support from NASA Award No. NNG04GJ90G and NSF Career Award No. Atm-0348819. Thanks are due to Warren Peters, the U.S. EPA/OAQPS, and George Pouliot, Ken Schere, and Tom Pierce, the U.S. NOAA/EPA, for providing meteorological fields, emission inventories, initial and boundary conditions for the July 2001 baseline simulations.

5. REFERENCES

Arnold, S. R., D. V. Spracklen, J. Williams, N. Yassaa, J. Sciare, et al. (2008), Evaluation of the global oceanic isoprene source and its impacts on marine organic carbon aerosol, *Atmos. Chem. Phys. Discuss*, 8, 16445-16471.

Blondeau-Patissier, D., G. H. Tilstone, V. Martinez-Vicente, and G. F. Moore (2004), Comparison of bio-physical marine products from SeaWiFS, MODIS, and a bio-optical model with in situ measurements from Northern European waters, *J. Opt. A: Pure Appl. Opt.*, 6, 875-889.

Butler, J. H., D. B. King, J. M. Lobert, S. A. Montzka, S. A. Yvon-Lewis, B. D. Hall, N. J. Warwick, D. J. Mondeel, M. Aydin, and J. W. Elkins (2007), Oceanic distributions and emissions of short-lived halocarbons, *Global Biogeochem. Cycles*, 21, GB1023, doi:10.1029/2006GB002732.

Claeys, M.B., Graham, G. Vas, W. Wang,R. Vermeylen, V. Pashynska et al. (2004), Formation of Secondary organic aerosols through photooxidation of isoprene, *Science*, 303, 1137.

Edney E.O., T.E. Kleindienst, M. Jaoui, M. Lewandowski, J.H. Offenberg, W. Wang, M. Claeys (2005), Formation of 2-methyl tetrols and 2-methylglyceric acid in secondary organic aerosol from laboratory irradiated isoprene/NO_X/SO_2/air mixtures and their detection in ambient $PM_{2.5}$ samples collected in the eastern United States, *Atmos. Environ.*, 39, 5281-5289.

Ervens B., A. G. Carlton, B. J. Turpin, K. E. Altieri, S. M. Kreidenweis, and G. Feingold

(2008), Secondary organic aerosol yield from cloud-processing of isoprene oxidation products, *Geophys. Res. Let.*, Vol. 35, L02816, doi:10.1029/2007GL031828, 2008

Greenberg J. P., A. B. Guenther, and A. Turnipseed (2005), Marine Organic Halide and Isoprene Emissions Near Mace Head, Ireland,

Guenther, A., C. N. Hewitt, D. Erickson, R. Fall, C. Geron, and T. Gracdcl et al. (1995), A global model of natural volatile organic compound emissions, *J. Geophys. Res.*, 100, 8873-8892.

A. Guenther, T. Karl, P. Harley, C. Wiedinmyer, P. I. Palmer, and C. Geron (2006), Estimates of global terrestrial isoprene emissions using MEGAN (Model of Emissions of Gases and Aerosols from Nature), *Atmos. Chem. Phys.*, 6, 3181–3210, 2006

Kroll, J. H., N. L. Ng, S. M. Murphy, R. C. Flagan, and J. H. Seinfeld (2006), Secondary organic aerosol formation from isoprene photooxidation, *Environ. Sci. Technol.*, 40, 1869 – 1877, doi:10.1021/es0524301.

Liakakou, E., M. Vrekoussis, B. Bonsang, C. Donousis, M. Kanakidou, and N. Mihalopoulos (2007), Isoprene above the Eastern Mediterranean: Seasonal variation and contribution to the oxidation capacity of the atmosphere, *Atmos. Environ.*, 41, 1002-1010.

Matsunaga, S., M. Mochida, T. Saito, and K. Kawamura (2002), In situ measurement of isoprene in the marine air and surface seawater from the western North Pacific, *Atmos. Environ.*, 36, 6051-6057.

Meskhidze, N., and A. Nenes (2006), Phytoplankton and cloudiness in the Southern Ocean, *Science*, 314, doi:10.1126/science.1131779

Ng, N. L., A. J. Kwan, J. D. Surratt, A. W. H. Chan, P. S. Chhabra, and A. Sorooshian et al. (2008), Secondary organic aerosol (SOA) formation from reaction of isoprene with nitrate radicals (NO_3), *Atmos. Chem. Phys.*, 8, 4117–4140, 2008

Palmer, P. I., and S. L. Shaw (2005), Quantifying global marine isoprene fluxes using MODIS chlorophyll observations, *J. Geophys. Res*., 32, L09805, doi:10.1029/2005GL022592

Pankow, J. (1994), An absorption model of the gas/aerosol partitioning involved in the formation of secondary organic aerosols, *Atmos. Environ.*, Vol. 28, No. 2, 189-193.

Park, R. J., D. J. Jacob, B. D. Field, R. M. Yantosca, and M. Chin (2004), Natural and transboundary pollution influences on sulfate-nitrate-ammonium aerosols in the United States: Implications for policy, *J. Geophys. Res.*, 109, D15204, doi:10.1029/2003JD004473.

Shaw, S. L., S. W. Chisholm, and R. G. Prinn (2003), Isoprene production by Prochlorococcus, a marine cyanobacterium, and other phytoplankton, *Mar. Chem.*, 80, 227-245.

Sinha, V., J. Williams, M. Meyhofer, U. Riebesell, A. I. Paulino, and A. Larsen (2007), Air-sea fluxes of methanol, acetone, acetaldehyde, isoprene and DMS from a Norwegian fjord following a phytoplankton bloom in a mesocosm experiment, *Atmos. Chem. Phys*., 7, 739-755.

Zhang, Y., J. Huang, D. Henze, and J. Seinfeld (2007), Role of isoprene in secondary organic aerosol formation on a regional scale, *J. Geophys. Res*. 112, D20207, doi:10.1029/2007/JD008675.